Molecular Microbiology (2012) 86(4), 882–893 ■
doi:10.1111/mmi.12023
First published online 18 September 2012

Crystal structure of the MrkD$_{1P}$ receptor binding domain of *Klebsiella pneumoniae* and identification of the human collagen V binding interface

Ana Toste Rêgo,[1†] Jeremiah G. Johnson,[2‡] Sebastian Geibel,[1] Francisco J. Enguita,[3] Steven Clegg[2] and Gabriel Waksman[1,4*]

[1]*Institute of Structural and Molecular Biology* at *University College London and Birkbeck College, Malet Street, London WC1E 7HX, UK.*

[2]*Department of Microbiology, College of Medicine, University of Iowa, Iowa City, Iowa, 52242, USA.*

[3]*Instituto de Medicina Molecular, Faculdade de Medicina, Universidade de Lisboa, Lisboa, Portugal.*

[4]*Research Department of Structural and Molecular Biology, University College London, Gower Street, WC1E 6BT, UK.*

Summary

Klebsiella **species are members of the family enterobacteriaceae, opportunistic pathogens that are among the eight most prevalent infectious agents in hospitals. Among other virulence factors in** ***Klebsiella*****, type 3 pili exhibit a unique binding pattern in the human kidney via interaction of two MrkD adhesion variants 1C1 and 1P to type IV and/or V collagen. However, very little is known about the nature of this recognition. Here we present the crystal structure of the plasmid born MrkD$_{1P}$ receptor domain (MrkDrd). The structure reveals a jelly-roll β-barrel fold comprising 17 β-strands very similar to the receptor domain of GafD, the tip adhesin from the F17 pilus that recognizes N-acetyl-D-glucosamine (GlcNAc). Analysis of collagen V binding of different MrkD$_{1P}$ mutants revealed that two regions were responsible for its binding: a pocket, that aligns approximately with the GlcNAc binding pocket of GafD involving residues R105 and Y155, and a transversally oriented patch that spans strands β2a, β9b and β6 including residues V49, T52, V91, R102 and I136. Taken together, these data provide structural and functional insights on MrkD$_{1P}$ recognition of host cells, providing a tool for future development of rationally designed drugs with the prospect of blocking** ***Klebsiella*** **adhesion to collagen V.**

Accepted 29 August, 2012. *For correspondence. E-mail g.waksman@bbk.ac.uk or g.waksman@ucl.ac.uk; Tel. (+44) 020 7631 6833; Fax (+44) 020 7631 6803. Present addresses: †MRC Laboratory of Molecular Biology, Hills Road, Cambridge CB2 0QH, UK; ‡Department of Microbiology and Immunology, University of Michigan, Ann Arbor, Michigan, 48109, USA.

Introduction

Klebsiella pneumoniae is frequently associated with hospital-acquired urinary tract infections (UTI), pneumonia, septicaemia, and wound infections. Among other virulence factors, *Klebsiella* strains express Mrk type 3 pili, which protrude as hair-like fibres from the bacterial surface and exhibit a unique binding pattern in the human kidney. On their tip, Mrk pili can display different variants of an adhesin protein MrkD that specifically interact with type IV and/or V collagen present in tubular basement membranes, Bowman's capsule, arterial walls, and the interstitial connective tissues of the kidney (Furthmayr and Madri, 1982; Martinez-Hernandez *et al.*, 1982; Modesti *et al.*, 1984; Tarkkanen *et al.*, 1990; 1998; Sebghati and Clegg, 1999). Recognition of extracellular matrix components such as collagens, fibronectin, fibrinogen or laminin by adhesins is far from unique. For instance Dr fimbriae mediate *Escherichia coli* binding to type IV collagen (Westerlund *et al.*, 1989a), FimH from type 1 pili in meningitis associated *E. coli* binds to collagen Type I and IV (Pouttu *et al.*, 1999) and the minor subunits PapE and PapF from P pili have been shown to mediate binding to fibronectin (Westerlund *et al.*, 1989b; 1991).

Electron microscopy showed that Mrk pili are thin flexible fibres, 2–4 nm wide and 0.5–2 μm long (Hornick *et al.*, 1995) which are made up of repeated MrkA subunits (the major subunit), the minor subunit MrkF inserted intermittently between MrkA subunits (Huang *et al.*, 2009) and the adhesin MrkD at the distal end of the pilus (Tarkkanen *et al.*, 1998) (Fig. S1A). Protein sequence alignments and biochemical studies indicate that MrkD comprises a N-terminal collagen V binding domain, here referred to as receptor binding domain or MrkDrd (Sebghati and Clegg, 1999), and a C-terminal pilin domain that connects the adhesin with the next subunit in the pilus (Girardeau and Bertin, 1995). Three alleles of *mrkD* (1P, 1C1, 1C2) have been described in *Klebsiella* (Sebghati *et al.*, 1998).

Adhesin $MrkD_{1P}$ is encoded by plasmids that are found in most strains of *Klebsiella oxytoca* and a minority of *Klebsiella pneumoniae* strains while alleles *mrkD*$_{1C1}$ and *mrkD*$_{1C2}$ are encoded in the genome of *Klebsiella pneumoniae*. When assembled into the pilus, $MrkD_{1P}$ mediates adherence to type V collagen, whereas $MrkD_{1C1}$ binds to type IV and V collagens (Tarkkanen *et al.*, 1990; Sebghati *et al.*, 1998). $MrkD_{1C2}$ causes the typical *Klebsiella*-like D-mannose-resistant haemagglutination (HA) of tannic acid treated erythrocytes indicating adherence property (Clegg and Gerlach, 1987) but it neither binds to type IV or type V collagen (Sebghati *et al.*, 1998).

Mrk pilus subunits are encoded by the *mrk* gene cluster alongside regulatory genes for Mrk pilus expression (Allen *et al.*, 1991) (Fig. S1B). Protein sequence comparisons showed that the Mrk pilus system belongs to the family of chaperone–usher assembled pili (Nuccio and Baumler, 2007) that are represented by the well-studied P and type 1 pili (Geibel and Waksman, 2011). Therefore, it is assumed that Mrk pili are anchored to the outer bacterial membrane by their assembly platform, the usher MrkC. In the periplasm, the chaperone MrkB presumably catalyses the folding of Mrk pilus subunits, stabilizes them and recruits them to the usher for pilus assembly (Fig. S1A).

Because structures of the MrkD variants are unknown, very little is understood about the nature of their interaction with collagen IV or V. Here we report the crystal structure of the $MrkD_{1P}$ receptor binding domain (MrkDrd) and identify its collagen V binding site by site-directed mutational analysis.

Results

The receptor binding domain of $MrkD_{1P}$ is resistant to trypsinization

Because attempts to crystallize the chaperone : adhesin complex MrkB : $MrkD_{1P}$ (UniProtKB/Swiss-Prot code for $MrkD_{1P}$ P21648) were unsuccessful, the protein complex was subjected to limited proteolysis. Three main fragments were obtained (bands 1 to 3 in Fig. S2). Edman sequencing identified the top fragment (band 1 in Fig. S2) as being a mixture of the N-terminal $MrkD_{1P}$ receptor binding domain and the C-terminal $MrkD_{1P}$ pilin domain, the N-terminus of which started at residue 199. The molecular weight of the proteolysis products was in accordance with the expected boundary between the $MrkD_{1P}$ receptor binding and pilin domains estimated by protein sequence comparisons with the structurally known adhesins FimH and PapG (Fig. S3). Subsequently the region of the *mrkD*$_{1P}$ gene (GenBank Code M24536.1) encoding residues 21–198 was cloned, expressed in *E. coli* BL21 and MrkDrd purified and crystallized (*Experimental procedures*; Fig. S4).

Table 1. Data collection, phasing and refinement statistics.

	Peak (SeMet)
Data collection statistics	
Space group	$P3_121$
Number of molecules in *a.u.*	1
Resolution (Å)[a]	41.81–3.0 (3.16–3.0)
Wavelength (Å)	0.9792
Cell dimensions	
a (Å)	49.81
b (Å)	49.81
c (Å)	169.93
α (°)	90
β (°)	90
γ (°)	120
Total number of hkl[a]	108975 (16161)
Number of unique hkl[a]	5246 (748)
Overall multiplicity[a]	20.8 (21.6)
R_{merge}[a,b]	0.108 (0.609)
Average I/σ(I)[a]	23.9 (6.2)
% overall completeness[a]	98.7 (98.6)
Refinement Statistics	
Resolution range (Å)	56.64–3.0
Mean B value (Å^2)	69.51
Mean Wilson B value (Å^2)	71.62
R_{work}/R_{free}[c,d]	22.7/27.3
RMSD bond lengths (Å)	0.005
RMSD bond angles (Degrees)	0.87
Ramachandran plot (%)[e]	98.1/1.9/0.0

a. Values in parentheses refer to the highest resolution shell.

b. $R_{merge} = \sum_{hkl}\sum_i |I_i(hkl) - \overline{I(hkl)}| \Big/ \sum_{hkl}\sum_i I_i(hkl)$

c. $R_{work} = \sum_{hklCW} ||F_{obs}| - k|F_{calc}|| \Big/ \sum_{hklCW} |F_{obs}|$, where W is the working set.

d. $R_{free} = \sum_{hklCT} ||F_{obs}| - k|F_{calc}|| \Big/ \sum_{hklCT} |F_{obs}|$, where T is the test set obtained by randomly selecting 5% of the data.

e. Residues in favoured/allowed/outlier regions of the Ramachandran plot calculated with MOLPROBITY (Chen *et al.*, 2010a).

Structure determination of MrkDrd

The crystal structure of MrkDrd was determined to a resolution of 3.0 Å. The phase problem was solved by single anomalous dispersion (SAD) (Table 1) using four selenomethionines in the asymmetric unit of the crystal (Fig. S5; *Experimental procedures*). After the refinement process, a model of MrkDrd was built comprising 90.4% of its amino acid sequence. Electron density could not be interpreted for a part of the N-terminal Strep-tag. At the C-terminus, the last C-terminal residue visible in the electron density was L181.

MrkDrd and other adhesin domains share a jelly-roll β-barrel fold but present different receptor binding sites

MrkDrd shows a jelly-roll β-barrel fold comprising 17 β-strands (1a, 1b, 1c, 2a, 2b, 3, 4, 5, 6, 7, 8, 9a, 9b, 10a, 10b, 11a, 11b) (Fig. 1A). MrkDrd has a compact elongated shape with dimensions of 54.2 Å × 23.8 Å × 18.3 Å and a disulfide bridge between C22 (β1a) and C67 (β2b) that presumably confers rigidity to the structure and helps to

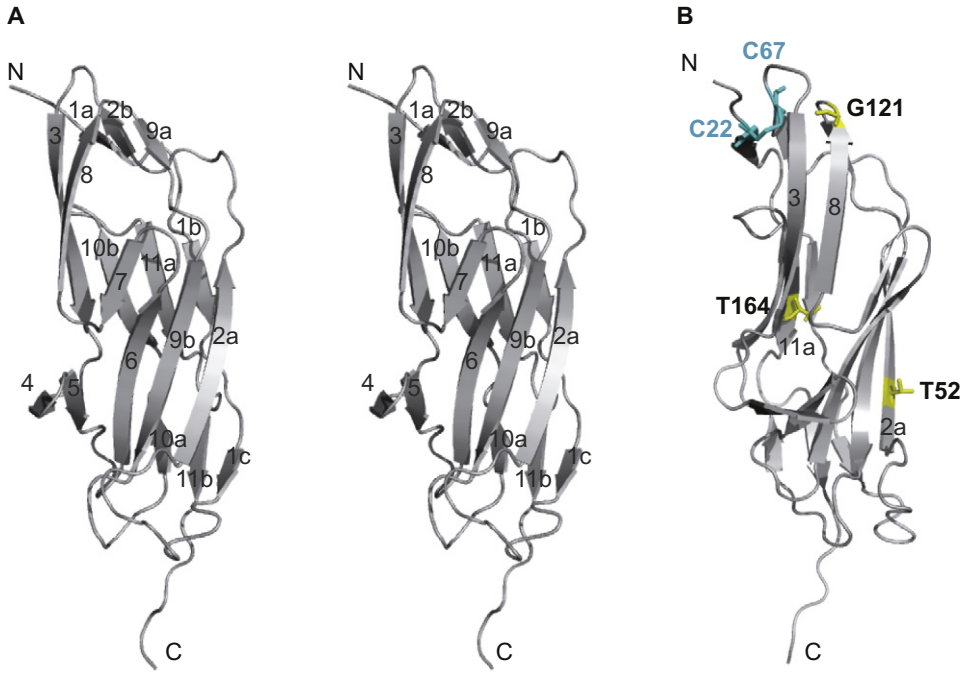

Fig. 1. Crystal structure of the $MrkD_{1P}$ receptor binding domain.
A. Stereo view in ribbon representation of the model of $MrkD_{1P}$ receptor binding domain. β strands are numbered 1–11.
B. View of the MrkDrd structure showing the disulfide bridge between C22 and C67 coloured in blue and residues T52, G121 and T164 that were examined in a previous study (Sebghati and Clegg, 1999) in yellow and stick representation. This figure is available in colour online at wileyonlinelibrary.com.

stabilize a rather flexible N-terminus (Fig. 1B). A deep pocket is observed near the N-terminus (defined as the 'top' of the structure; clearly visible in Fig. 3B).

Structure comparisons with the receptor binding domains of adhesins GafD (F17c-type and F17a-G) (pdb 1OIO and pdb 1O9W respectively), FimH (pdb 1TR7) and PapG (pdb 1J8R) (Dodson *et al.*, 2001; Buts *et al.*, 2003; Merckel *et al.*, 2003; Bouckaert *et al.*, 2005) showed that MrkDrd is most related to GafDrd/F17-G [Z score of 9.5 and root-mean square deviation (RMSD) of 4.1 Å for 141 C_α-positions] (Fig. 2), despite amino acid sequence homology of < 11% (sequence identity) (Holm *et al.*, 2008). Alignment of the receptor binding domain structures of FimH and PapG with MrkDrd yielded lower Z scores of 4.1 and 3.3 and RMSD of 4.3 Å and 4.4 Å for 119 and 103 C_α-positions respectively.

The receptor binding domains of adhesins $MrkD_{1P}$, GafD/F17-G, FimH and PapG share a jelly-roll β-barrel fold (Figs 2 and S6). The receptor binding sites for GafD, FimH and PapG have been identified but locate in a very different region in each of the structures (Fig. S6): the D-mannopyranoside binding site of FimH is a deep negatively charged pocket at the tip of the receptor binding domain (Adams *et al.*, 2002), the Gal(α1–4)Gal binding site of PapG is a shallow pocket on the side of the molecule (Dodson *et al.*, 2001) and GafD/F17-G binds N-acetyl-D-glucosamine (GlcNAc) in a shallow pocket on top of the receptor binding domain (Buts *et al.*, 2003; Merckel *et al.*, 2003). This, together with the fact that sugar binding has not been described for any of the MrkD variants, suggests that the structural comparison of MrkDrd with the receptor binding domains of GafD, FimH or PapG might not provide helpful clues as to where the collagen binding site of MrkDrd might be located.

A hydrophobic patch composes the collagen V binding site on the $MrkD_{1P}$ receptor binding domain

To identify the collagen V binding site on MrkDrd we mutated 16 solvent exposed amino acids in various regions of the MrkDrd structure and measured their impact on collagen V binding (Fig. 3A and B, and *Experimental procedures*). These mutants aim to test most surfaces of MrkDrd. Among other mutations, substitutions to Gly were introduced and tested. These mutations were either in loops or β-strands and therefore would not be expected to be structurally disruptive (see http://www.bmrb.wisc.edu/referenc/choufas.html and associated references). The collagen V binding assay was carried out using *E. coli* HB101 that contains plasmid pFK68Δ*mrkD*$_{1P}$ encoding all Mrk proteins for pilus assembly except for adhesin $MrkD_{1P}$ and was transformed with empty plasmid pTrc99A (negative control) or with plasmid pTrc99A*mrkD*$_{1P}$ encoding either wild type $MrkD_{1P}$ (positive

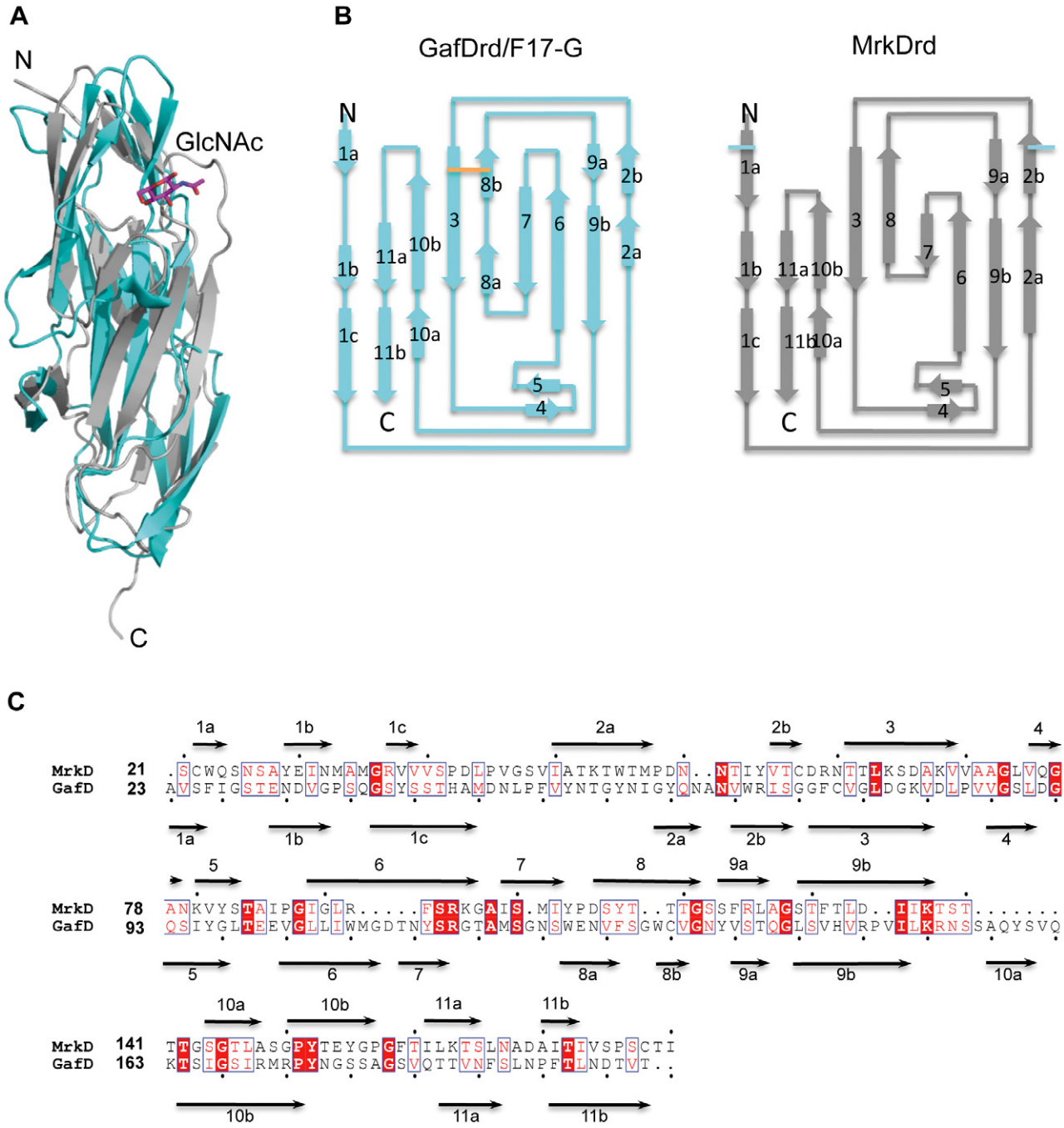

Fig. 2. Comparison of the receptor binding domain structures of adhesins MrkD$_{1P}$ and GafD.
A. Structure alignment of MrkD$_{1P}$ receptor binding domain (grey) and GafD receptor binding domain (light blue) bound to GlcNAc (magenta).
B. Topology diagrams of MrkD$_{1P}$ receptor binding domain (grey) and GafD receptor binding domain (light blue). Lines in orange (GafDrd) and light blue (MrkDrd) represent the location of the disulfide bridge in the two domains.
C. Sequence alignment of the MrkD$_{1P}$ and GafD receptor binding domains. The secondary structure elements for MrkD$_{1P}$ and GafD receptor binding domains are represented on the top and bottom of the protein sequences. Numbering for both protein sequences is indicated. Alignment was generated by ClustalW (Larkin *et al.*, 2007) and conservation of amino acids visualized by the ESPript server (Gouet *et al.*, 1999). White characters in red boxes represent strict amino acid identity, red characters represent type conserved amino acid substitutions and a blue frame represent semi-conserved amino acid substitutions. This figure is available in colour online at wileyonlinelibrary.com.

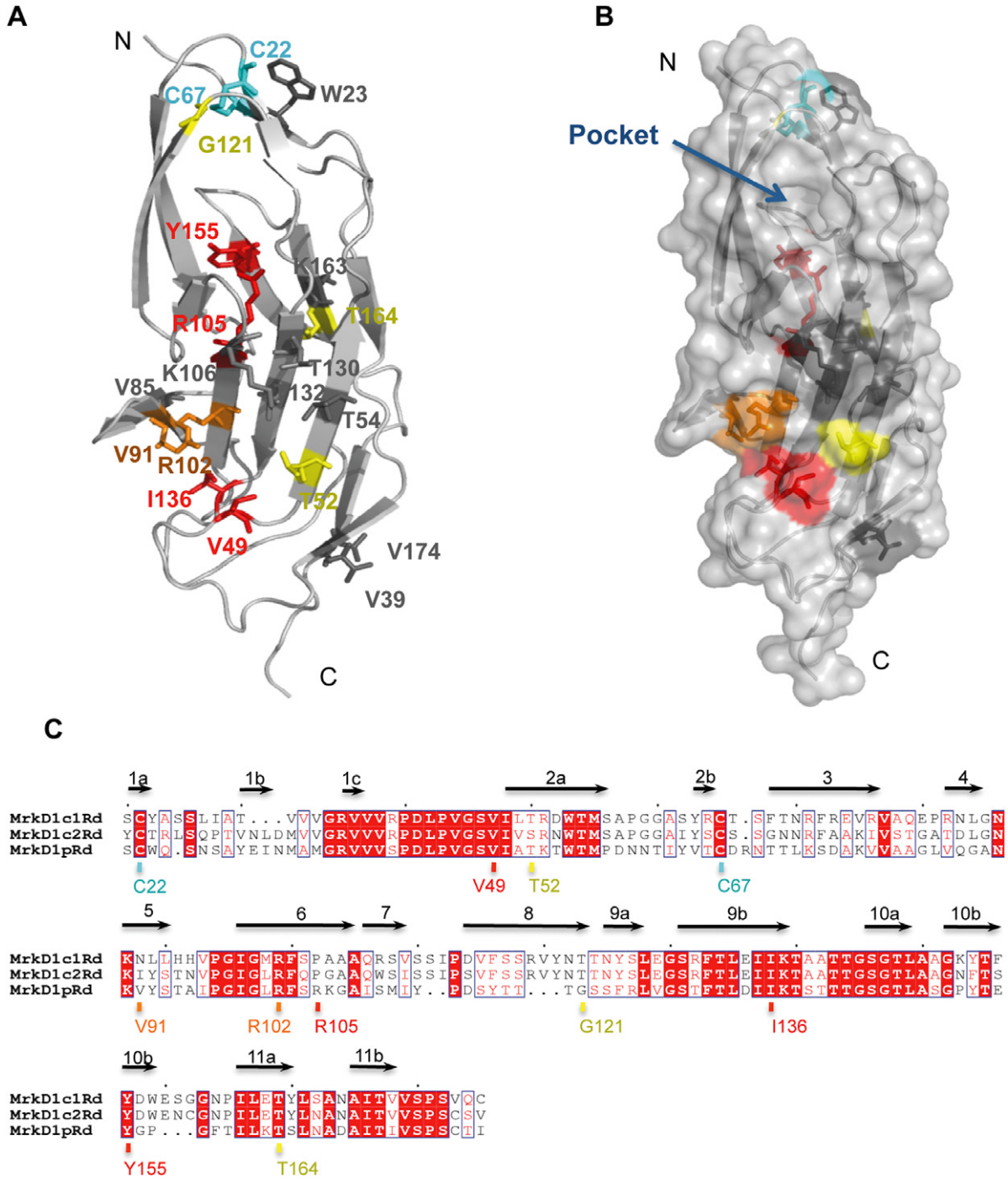

Fig. 3. Localization of residues mutated on the MrkDrd structure.
A. MrkDrd structure as ribbon representation is showing mutated residues as stick model. Residues are colour schemed for its effect on collagen V binding. In yellow (T52, G121 and T164) are represented the residues first described by Sebghati and collaborators as residues involved in collagen V binding (Sebghati and Clegg, 1999). Mutagenesis of residues in red (V49, R105, I136 and Y155) abolished collagen V binding in this study. Mutagenesis of residues in orange (V91 and R102) affected collagen V binding severely. Residues in grey (W23, V39, T54, V85, K106, T130, T132, K163 and V174) did not have an effect on collagen V binding upon mutagenesis. The disulfide bridge between C22 and C67 is shown in blue.
B. Surface representation of the MrkDrd structure shown in panel A with same colour-coding of residues. The arrow points to the deep pocket identified as one of the two collagen binding sites.
C. Protein sequence alignment of the receptor binding domain of adhesin variants $MrkD_{1P}$, $MrkD_{1C1}$ and $MrkD_{1C2}$. Residues mutated in $MrkD_{1P}$ shown to affect collagen V binding are numbered and maintain the same colour scheme. Cysteines forming disulfide bridges are also listed and coloured in cyan. This figure is available in colour online at wileyonlinelibrary.com.

Table 2. Type 3 pilus surface expression and haemagglutination of tannic acid-treated bovine erythrocytes.

E. coli strain (plasmid)	Type 3 pilus expression	Haemagglutination
HB101 (pFK68)	++++	+++
HB101 (pFK68Δ*mrkD*)	–	–
HB101 (pFK68Δ*mrkD*) (pTrc99*mrkD*)	++++	+++
HB101 (pFK68Δ*mrkD*) (pTrc99A)	–	–
HB101 (pFK68Δ*mrkD*) (pTrc99$mrkD_{W23A}$)	++++	+++
HB101 (pFK68Δ*mrkD*) (pTrc99$mrkD_{V39G}$)	++++	+++
HB101 (pFK68Δ*mrkD*) (pTrc99$mrkD_{V49G}$)	++++	–
HB101 (pFK68Δ*mrkD*) (pTrc99$mrkD_{V49A}$)	++++	+++
HB101 (pFK68Δ*mrkD*) (pTrc99$mrkD_{T52A}$)	++++	+++
HB101 (pFK68Δ*mrkD*) (pTrc99$mrkD_{T52S}$)	++++	+++
HB101 (pFK68Δ*mrkD*) (pTrc99$mrkD_{T54A}$)	++++	+++
HB101 (pFK68Δ*mrkD*) (pTrc99$mrkD_{V85G}$)	++++	+++
HB101 (pFK68Δ*mrkD*) (pTrc99$mrkD_{V91G}$)	++++	–
HB101 (pFK68Δ*mrkD*) (pTrc99$mrkD_{R102G}$)	++++	+ (weak)
HB101 (pFK68Δ*mrkD*) (pTrc99$mrkD_{R105E}$)	++++	–
HB101 (pFK68Δ*mrkD*) (pTrc99$mrkD_{K106A}$)	++++	+++
HB101 (pFK68Δ*mrkD*) (pTrc99$mrkD_{T130A}$)	++++	+++
HB101 (pFK68Δ*mrkD*) (pTrc99$mrkD_{T132A}$)	++++	+++
HB101 (pFK68Δ*mrkD*) (pTrc99$mrkD_{I136G}$)	++++	–
HB101 (pFK68Δ*mrkD*) (pTrc99$mrkD_{I136A}$)	++++	–
HB101 (pFK68Δ*mrkD*) (pTrc99$mrkD_{Y155A}$)	++++	–
HB101 (pFK68Δ*mrkD*) (pTrc99$mrkD_{Y155F}$)	++++	–
HB101 (pFK68Δ*mrkD*) (pTrc99$mrkD_{K163A}$)	++++	+++
HB101 (pFK68Δ*mrkD*) (pTrc99$mrkD_{V174G}$)	++++	+++

control) or $MrkD_{1P}$ variants (*Experimental procedures*). Collagen V binding of *E. coli* HB101 double transformants was quantified by enzyme-linked immunosorbent assay (ELISA) (*Experimental procedures*). Furthermore, expression of Mrk pili on the bacterial surface was examined by serum agglutination and adherence of $MrkD_{1P}$ variants by HA of tannic acid-treated bovine erythrocytes (*Experimental procedures*).

Of 20 *E. coli* HB101 strains encoding $MrkD_{1P}$ pilus variants, nine strains (W23A, V39G, T54A, V85G, K106A, T130A, T132A, K163A and V174G) showed pilus expression, HA and collagen V binding activities comparable to the wild type control showing that these residues are not involved in collagen V binding (Table 2; Fig. 4). *E. coli* HB101 harbouring plasmids pFK68Δ$mrkD_{1P}$ and pTrc99A without $mrkD_{1P}$ insert (negative control) were not piliated

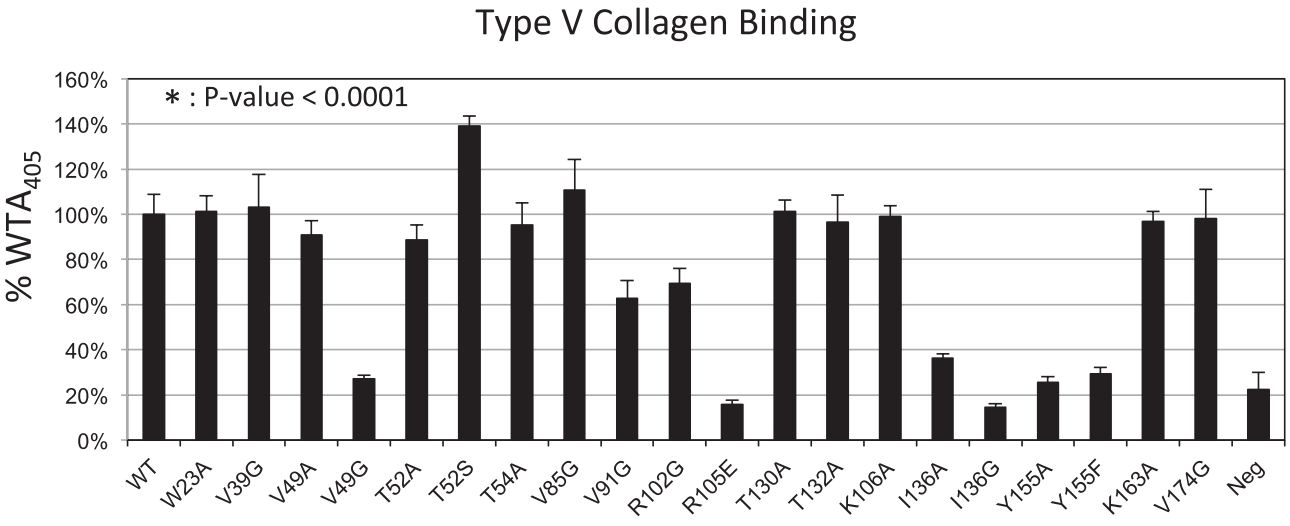

Fig. 4. Effect of $MrkD_{1P}$ mutations on collagen V binding ability. Bars show collagen V binding activity of $MrkD_{1P}$ variants or wild type $MrkD_{1P}$ incorporated into Mrk pili expressed by *E. coli* HB101. Wild type $MrkD_{1P}$ represents 100% collagen V binding activity. Statistical analyses were performed using a two-tailed Students *t*-test.

and consequently did not exhibit HA activity nor collagen V binding showing that Mrk pilus assembly is dependent on incorporation of $MrkD_{1P}$ into the pilus tip. The remaining 11 *E. coli* HB101 strains expressing $MrkD_{1P}$ variants V49G, V49A, T52A, T54S, V91G, R102G, R105E, I136G, I136A, Y155F and Y155A produced pili at wild type level but the mutations affected HA (Table 2) and collagen V binding activity (Fig. 4) demonstrating that these residues are involved in collagen V binding.

Collagen V binding amino acids cluster around two regions on MrkDrd, a deep pocket, where residues R105 and Y155 are found at the bottom, that aligns approximately with the GlcNAc binding site of GafD, and a transversally oriented patch that spans strands β2a, β9b and β6 including residues V49, T52, V91, R102 and I136 (Fig. 3A and B). Residues V49 and I136 make up the hydrophobic core of the binding patch on MrkDrd and are surrounded by residues T52, V91 and R102 (Fig. 3A). When mutated to alanine, residue V49 still mediates HA of tannic acid treated erythocytes (Table 2), but collagen V binding activity of $MrkD_{1P}$ is decreased to 90%. In contrast, $MrkD_{1P}$ variant I136A could not trigger HA and its collagen V binding activity was only 40% of the wild type $MrkD_{1P}$ (Table 2). The influence of hydrophobicity of the hydrophobic patch on collagen V binding of $MrkD_{1P}$ became more apparent when residues V49 and I136 were mutated to glycine in order to exclude the hydrophobic effect that the alanine methyl side-chain exerts. This time, both $MrkD_{1P}$ variants V49G and I136G failed to mediate HA (Table 2). Collagen V binding activity of $MrkD_{1P}$ variant V49G was reduced even further to 30% of the wild type $MrkD_{1P}$ level while collagen V binding activity of variant I136G did not exceed the basal level of the negative control (*E. coli* HB101 transformed with plasmids pFK68Δ*mrkD*$_{1P}$ and pTrc99A without insert) (Fig. 4). $MrkD_{1P}$ variants V91G and R102G showed less HA activity compared with wild type $MrkD_{1P}$ (Table 2) and their ability to bind collagen V corresponded to ~ 65% and ~ 70% respectively of wild type $MrkD_{1P}$ level (Fig. 4). Mutation of residue T52 to the more hydrophobic and bulkier isoleucine was reported in a previous study to abolish collagen V binding of piliated bacteria expressing this $MrkD_{1P}$ variant (Sebghati and Clegg, 1999). Residue T52 lies in a stretch of conserved amino acids among all three MrkD (1C1, 1C2 and 1P) variants and is conserved between $MrkD_{1C1}$ and $MrkD_{1P}$ (Fig. 3C). However, in the amino acid sequence of the inactive $MrkD_{1C2}$ variant a serine is found in position 52. Since this is only a small change in an otherwise conserved stretch of the amino acid sequence and given the fact that variant T52I can eliminate collagen V binding of $MrkD_{1P}$, we tested weather a T52S mutation could also abolish collagen V binding of $MrkD_{1P}$. Surprisingly, $MrkD_{1P}$ variant T52S showed increased collagen V binding activity by 40% while mutation T52A did not affect collagen V binding. The mutagenesis of T52 to S, A or I shows, that collagen V binding of $MrkD_{1P}$ is sensitive to small side-chain changes of T52.

Mutations at the structure's bottom (V39G, V174G), top (W23A), backside (K163A), face (T54A, K106A, T130A and T132A) or on a potential extension of the hydrophobic patch (V85G) were carried out to delimit the collagen V binding site of MrkDrd and showed HA and collagen V binding activities comparable to that of wild type $MrkD_{1P}$ indicating that these residues do not contribute to collagen V binding (Table 2; Figs 3A and 4). The non-collagen V binding residues T54, T130, T132, K106 lie in between the collagen V binding hydrophobic patch and the small pocket of MrkDrd. There is no direct connection of collagen V binding residues from the hydrophobic patch to the small pocket on MrkD. Thus, collagen V must be bound by two distinct sites of the MrkDrd.

The transversally oriented receptor binding patch on MrkDrd has an estimated area of approximately 80 $Å^2$ (~ 16 Å length and ~ 5 Å width) and therefore meets the requirement for binding a fibre shaped molecule like a collagen V triple helix. Interestingly, collagen V binding residues V49, V91 and I136 of $MrkD_{1P}$ are structurally conserved in GafD (V127, V31, I73; GafD numbering) but their function has not been examined nor has collagen binding been described for GafD/F17-G.

The MrkDrd crystal structure also revealed the structural basis for the effects of mutations G121D and T164I shown in a previous study to abolish collagen V binding of $MrkD_{1P}$ (Fig. 1B) (Sebghati and Clegg, 1999): indeed, mutation of G121D abolishes the flexibility that G121 confers to a short loop between β-strands β8 and β9a and will therefore hamper the correct folding of MrkDrd, while residue T164 is buried in the core of the molecule and mutation to isoleucine will most likely destabilize the MrkDrd fold.

A deep pocket on the $MrkD_{1P}$ receptor binding domain also affects the binding of collagen V

Our study revealed a deep pocket at the top of the molecule (Fig. 3B) as a potential collagen V binding site on MrkDrd. This pocket is lined at the bottom by the hydroxyl group of Y155 and the guanidinium group of R105. This pocket is too small to recognize larger parts of the collagen V triple helix structure. Therefore, we suspected that a single side-chain of collagen V (possibly a negatively charged residue given the positively charged nature of the pocket) could be inserted into the MrkDrd pocket. To test this hypothesis, mutations R105E, Y155A and Y155F were introduced and their ability to bind collagen V tested. All *E. coli* HB101 transformants expressed Mrk pili but the mutations R105E, Y155A and Y155F of MrkDrd clearly affected HA and collagen V binding activities (Table 2;

Fig. 4). Mutations Y155A and Y155F abolished HA activity of $MrkD_{1P}$ and decreased its collagen V binding activity to ~ 30% of the wild type $MrkD_{1P}$ level (Table 2; Fig. 4). The effect on collagen V binding of mutation Y155A could also be attributed to structural destabilization of the MrkDrd pocket or even of the whole MrkDrd domain because the small methyl side-chain of Y155A cannot replace the bulky phenyl ring of Y155. However, removing the hydroxyl group of Y155 (Y155F mutation) had a similar effect on HA and collagen V binding activities of $MrkD_{1P}$ (Table 2; Fig. 4) like mutation Y155A, indicating that the polar hydroxyl group of Y155 is crucial for collagen V binding rather than its phenyl group. Because of its small size it seems unlikely that the missing hydroxyl group of mutant Y155F could destabilize the MrkDrd structure.

Replacement of the positively charged R105 by a negatively charged shorter glutamate in the pocket of MrkDrd abolished HA and collagen V binding activities (Table 2; Fig. 4). We cannot rule out that mutation R105E caused structural instability of the MrkDrd domain (Sebghati and Clegg, 1999). On the other hand, a negatively charged collagen residue like glutamate could be repulsed by an equally charged R105E in the MrkDrd pocket.

Discussion

Recognition of host receptors by bacterial surface-exposed adhesins is a critical event in bacterial infections. In the past decade extensive work has been carried out in order to understand the mechanisms of host recognition by bacterial pathogens. The three dimensional structure of the adhesin domain of $MrkD_{1P}$ and the identification of its collagen V binding sites reported here provide new insights into the nature of the type 3 pili host recognition by *Klebsiella* strains. In this study collagen V binding could be clearly assigned to two distinct sites on the receptor binding domain MrkDrd of adhesin $MrkD_{1P}$.

One collagen V binding site of MrkDrd is a hydrophobic patch located at the lower side of the molecule in a shallow region that shows some similarity to the hydrophobic collagen binding region on the N1 subdomain of CNA, a multidomain membrane embedded adhesin of Gram positive *Staphylococcus aureus* [Fig. S7; CNA (pdb 2F6A)] (Zong *et al.*, 2005). CNA embraces snuggly the collagen triple helix by two subdomains N1 and N2 ('collagen hug' model) that are connected by a long hydrophobic linker (Fig. S7). After collagen binding, the N1 and N2 subdomain 'hug' is enforced by a loop of subdomain N2, termed the 'latch', that inserts into the binding patch of the N1 subdomain (Fig. S7). This mechanism is similarly seen in *Staphylococcus epidermidis* SdrG adhesin binding to fibrinogen (Ponnuraj *et al.*, 2003) making it a rather common mechanism, at least in Gram positive bacteria.

According to the 'collagen hug' model, MrkD receptor and pilin domains would need to wrap around the collagen V triple helix. It was shown that mutagenesis of residues R195 (to Q) and H277 (to Y) of the pilin domain can abolish collagen V binding when $MrkD_{1P}$ is assembled into the Mrk pilus (Sebghati and Clegg, 1999). This result could point to a collagen hug model. However, missing structural information of the $MrkD_{1P}$ pilin domain prevents validation of this collagen binding mode, for example whether residues R195Q and H277Y are surface exposed and where these residues are located relative to MrkDrd.

The other collagen V binding site is a deep positively charged pocket at the top of MrkDrd and is well separated from the hydrophobic patch. This pocket could possibly accommodate a glutamate or aspartate residue of collagen V by formation of a salt bridge with R105 of MrkDrd. A similar collagen binding mode has been observed for the I domain of Integrin $\alpha2\beta1$ (pdb 1DZI) which binds collagen in a magnesium dependent manner (Emsley *et al.*, 2000). The crystal structure of the I domain of Integrin $\alpha2\beta1$ in complex with a collagen triple helix shows that the magnesium ion is co-ordinated in a small pocket of the I domain where the co-ordination of the metal sphere is completed by a glutamate of the collagen triple helix. A salt bridge between of a possible glutamate side-chain of collagen V and R105 of MrkDrd would be a variant of the I domain of Integrin $\alpha2\beta1$ collagen binding mode.

D-mannose dependent collagen I and IV binding was shown for a meningitis-associated *E. coli* strain IHE 3034. *E. coli* IHE 3034 expresses a FimH adhesin variant that like $MrkD_{1P}$ consists of a receptor binding and a pilin domain that is used to assemble the adhesin into the corresponding pilus. It was demonstrated that a single (natural occurring) mutation, S62A, on the FimH fimbrial receptor domain is critical for the adhesiveness of *E. coli* IHE 3034 to collagen I and IV (Pouttu *et al.*, 1999). However, no mutation on the pilin domain of FimH IHE 3034 has been found to affect collagen I and IV binding indicating that collagen is exclusively bound by the receptor domain of FimH IHE 3034. Structural comparison of MrkDrd and FimH (Fig. S8; pdb 1QUN) of a non-pathogenic *E. coli* K12 (highly homologous to variant FimH IHE 3034) shows that the receptor domains bind collagen on different sites (Fig. S8). In contrast to FimH IHE 3034, $MrkD_{1P}$ collagen V binding is sugar independent as the collagen V used for our binding assay is not glycosylated. This rules out a possible direct binding mode of $MrkD_{1P}$ to collagen V by glycosylated collagen V residues as it was observed for GafD (F17-G) binding to laminin containing GlcNAc (Saarela *et al.*, 1996).

MrkDrd collagen V binding cannot be assigned unambiguously to known collagen binding models nor could we exclude most of the models. The comparisons indicate

rather that $MrkD_{1P}$ collagen V binding could be based on a combination of different binding elements of the presented collagen binding models.

Piliated *Klebsiella* strains expressing $MrkD_{1C1}$ were shown to bind collagen IV and V whereas *Klebsiella* strains containing $MrkD_{1C2}$ mediated HA of tannic acid-treated erythrocytes but no collagen IV or V binding (Sebghati *et al.*, 1998). $MrkD_{1C2}$ functions as adhesin *in vitro* although its receptor remains unknown. Protein sequence alignment of the three known MrkD variants ($MrkD_{1C1}$, $MrkD_{1C2}$ and $MrkD_{1P}$) showed that residues V49, T52 (S52 in $MrkD_{1C1}$), R102 and I136 within the hydrophobic patch of MrkDrd are conserved and suggest that these residues are also involved in HA activity of $MrkD_{1C1}$ and $MrkD_{1C2}$ and in collagen V binding activity of the Mrk_{1C1} variant (Fig. 3C). Further studies will show if collagen IV binding of Mrk_{1C1} is also affected by residues V49, T52 (S52 in $MrkD_{1C1}$), I136 and R102 (MrkDrd numbering) or if an entirely different set of amino acids is required. They will also address whether additional amino acids determine the specificity for collagen IV in $MrkD_{1C1}$ or even prevent collagen V binding by $MrkD_{1C2}$.

Experimental procedures

Limited proteolysis of chaperone–adhesin complex MrkB–$MrkD_{1P}$

The MrkB–$MrkD_{1P}$ complex was concentrated to 1 mg ml^{-1} in buffer 20 mM Tris-HCl pH 8.0, 50 mM NaCl. Proteolysis was performed at a trypsin : MrkB–$MrkD_{1P}$ molar ratios of 1:100 ratio in a total volume of 100 µl per reaction. Samples were left to digest for 120 min and aliquots taken at times 5, 15, 30, 60 and 120 min after which SDS sample buffer was added to stop the reaction. Samples were boiled and separated in a NuPAGE gel (Fig. S2). Limited proteolysis of the MrkB–$MrkD_{1P}$ complex shows that digestion was almost complete after 2 h leaving three proteolysis resistant fragments. Bands 1, 2 and 3 were N-terminally sequenced by Edman degradation.

Molecular cloning of MrkDrd

The coding DNA sequence of the receptor binding domain of $MrkD_{1P}$ (residues 21–198) was molecularly cloned from plasmid pFK12 into expression plasmid pASK-IBA12 (IBA bioTAGnology) that encodes for an OmpA signal peptide to secret MrkDrd into the periplasm and a N-terminal Strep-tag followed by a thrombin cleavage site. MrkDrd comprising residues 21–198 was amplified using primers MrkD21_IBA12-f and MrkD198_IBA12-r (Table S1) and inserted into plasmid pASK-IBA12 using BsaI restriction site.

Expression and purification of MrkDrd

An overnight culture of *E. coli* BL21 harbouring *pASK-IBA12mrkDrd* was grown at 37°C in LB medium containing 100 µg ml^{-1} ampicillin (Amp). Overexpression of MrkDrd was induced by addition of anhydrotetracyclin (AHT) to a final concentration of 100 µg ml^{-1} for 3 h when A_{600} reached 0.6. Cells were harvested by centrifugation and the periplasmic fraction was extracted as follows. Cells were resuspended in extraction buffer 20 mM Tris-HCl pH 8.0, 5 mM Ethylenediaminetetraacetic acid (EDTA), 20% sucrose. After shaking at 4°C for 30 min $MgCl_2$ was added to a final concentration of 10 mM to the cell resuspension. Cells were centrifuged at 11.000 *g* for 20 min and the supernatant containing MrkDrd was dialysed against buffer 100 mM Tris-HCl pH 8.0, 150 mM NaCl, 1 mM EDTA, 5 mM Dithiothreitol (DTT). MrkDrd was purified on a strep-tactin sepharose affinity column applying a step gradient of 0 to 2.5 mM D-Desthiobiotin in 100 mM Tris-HCl pH 8.0, 150 mM NaCl, 1 mM EDTA, 5 mM DTT followed by a S75 gel filtration column (HiLoad™ 16/60 Superdex™ 75 prep grade column; GE Healthcare) in buffer 20 mM Tris-HCl pH 8.0, 50 mM NaCl, 1 mM EDTA, 5 mM DTT. MrkDrd was concentrated to 8 mg ml^{-1} for crystallization.

Production of selenometionine-containing MrkDrd

Methionine auxotrophic strain *E. coli* B834 was transformed with expression plasmid pASK_IBA12_*mrkDrd* and grown in SeMet™ medium (Molecular Dimensions) containing 100 µg ml^{-1} Amp and L-Selenomethionine (Across Organics) according to the manufacturers' protocols. When A_{600} of *E. coli* B834 reached 0.7–1.0 overexpression of SeMet MrkDrd was induced by addition of AHT for 3 h. SeMet-containing MrkDrd was purified as described above for native MrkDrd and concentrated to 7 mg ml^{-1} for crystallization.

Crystallization and X-ray data collection

MrkDrd and its SeMet derivative were crystallized by hanging drop vapour diffusion in drops of 0.5 µl protein and 0.5 µl precipitant and equilibrated against 100 µl of mother liquor in the reservoir at 20°C. MrkDrd and SeMet MrkDrd crystals grew to a maximum size of 0.13 mm × 0.11 mm × 0.09 mm with hexagonal shape in conditions that varied between 0.1 M Sodium Acetate pH 4.6 to pH 4.8 and 8% PEG 4000 to PEG 6000 and were cryo-protected with 25% ethylene glycol in mother liquor before freezing in liquid nitrogen.

Datasets were recorded for crystals of native MrkDrd and SeMet derivative at 0.976 Å and 0.9792 Å (12.662 keV) corresponding to the peak of the SeMet K absorption edge at 100 K with a ADSC Quantum 315r CCD detector on beamline ID29 at the ESRF, Grenoble. Images were processed using programs XDS (Kabsch, 1993) and SCALA (CCP4, 1994).

Structure determination of MrkDrd

Four selenium sites were located by Difference Patterson Methods in the asymmetric unit of the crystal and the phase problem was solved by SAD using PHENIX (Adams *et al.*, 2002). A polyalanine and polyglycine model consisting of 155 residues was built into the initial electron density by PHENIX AutoBuild (Adams *et al.*, 2002). The remaining model accounting for 161 residues was built manually in COOT

(Emsley and Cowtan, 2004) and refined by simulated annealing with PHENIX (Adams *et al.*, 2002) and restrained refinement with Refmac5 (CCP4, 1994) until convergence of R-factor to 22.7% and R-free to 27.3%. MOLPROBITY confirmed good stereochemistry with all φ and ψ torsion angles in allowed areas (Chen *et al.*, 2010b). Data collection, phasing, and refinement statistics are summarized in Table 1.

Bacterial plasmids, oligonucleotides, and DNA manipulations for HA and collagen V binding assays

The bacterial plasmids used in this study are listed in Table S2 and the oligonucleotides used are listed in Table S1. All strains were grown at 37°C using Luria–Bertani (LB) media supplemented with Ampicilin (100 μg ml^{-1}) and/or chloramphenicol (Cam) (25 μg ml^{-1}). Plasmid DNA preparations, restriction digests, and other enzymatic reactions were performed according to the manufacturers' protocols using commercially available materials.

Deletion of $mrkD_{1P}$ from pFK68

To determine whether $MrkD_{1P}$ is required for type 3 pilus production and to provide a background for the expression of *mrkD* alleles, $mrkD_{1P}$ was deleted from pFK68 by PCR using the outward facing primers Δ*mrkD*ForXhoI and Δ*mrkD*RevXhoI. PCR amplified pFK68Δ$mrkD_{1P}$ was gel extracted and digested at the incorporated XhoI site. Digested plasmid was recircularized and the deletion of $mrkD_{1P}$ was confirmed by sequence analysis using the University of Iowa DNA Facility. The resulting plasmid was introduced into *E. coli* HB101 and examined for type 3 pilus surface expression as previously described (Johnson and Clegg, 2010; Johnson *et al.*, 2011).

Construction of site-directed substitution mutants

Amino acid substitutions in $MrkD_{1P}$ were constructed by overlapping extension PCR. Briefly, 5′ fragments and 3′ fragments of $mrkD_{1P}$ were amplified from plasmid pFK68 using a combination of either primers 5′$mrkD_{1P}$BamHI and the appropriate reverse primer or the 3′$mrkD_{1P}$HindIII primer and the appropriate forward primer. Resulting fragments were then gel extracted and used as template in a second PCR where they were extended without primers initially, then amplified using the primer combination 5′$mrkD_{1P}$BamHI and 3′$mrkD_{1P}$HindIII. Reconstituted $mrkD_{1P}$s were then gel extracted and subcloned into the vector pGEM-T Easy. Successful mutation of $mrkD_{1P}$ was verified by sequence analysis using the University of Iowa DNA Facility. Determinants that were correct were excised using BamHI-HindIII and ligated into those respective sites in the expression vector pTrc99A.

Pilus expression and HA phenotypes of $MrkD_{1P}$ mutants

The mutated $mrkD_{1P}$ derivatives cloned into pTrc99A, as well as pTrc99A carrying wild type $mrkD_{1P}$ or empty pTrc99A, were introduced into *E. coli* HB101 pFK68Δ$mrkD_{1P}$. These double transformants were examined for their ability to produce surface-associated type 3 pili by serum agglutination. Serial twofold dilutions of monospecific anti-MrkA serum were used to detect type 3 pili on bacterial suspensions (1×10^8 cfu ml^{-1}; cfu, colony-forming units) in 50 μl volumes. Serum was raised against affinity-purified MrkA subunits as previously described (Johnson and Clegg, 2010). The lowest dilution of serum used in these assays was 1:20 and visible agglutination in microtitre plates was determined following incubation at 37°C for 60 min followed by 8 h at ambient temperature. Serum titres (reciprocal of the highest dilution causing agglutination) in Table 2 are reported as ++++ for bacteria exhibiting titres equal to or greater than 1280 and – for bacteria with titres less than 20. HA reactions were performed using tannic acid-treated bovine erythrocytes and bacterial suspensions (1×10^{10} cfu ml^{-1}) were prepared following growth on LB-Amp/Cam agar as previously described (Gerlach *et al.*, 1989). HA reactions are reported as +++ if the red cells were agglutinated within 60 s of mixing, + if a weak HA reaction was observed after 3–5 min of mixing and – for no visible HA after 10 min of mixing.

Binding of $MrkD_{1P}$ mutants to human type V collagen

Type V collagen binding assays were performed on these double transformants as previously described (Sebghati *et al.*, 1998). Briefly, wells were coated with approximately 1 pmol of human type V collagen (Sigma-Aldrich, St Louis, MO) overnight at 4°C (Tarkkanen *et al.*, 1990). Wells were subsequently washed with PBS + 0.05% Tween20 and blocked for 2 h at room temperature with PBS + 1% BSA. Following blocking, twofold dilutions of bacterial suspensions at an original A_{600} of 1.2 in PBS + 0.05% Tween20 were incubated for 2 h at room temperature in collagen-coated wells. Bacteria were obtained from overnight LB-Amp/Cam broth cultures and examined for type 3 pilus production. Bound bacterial cells were detected using an anti-MrkA primary antibody at a 1:500 dilution in PBS + 0.05% Tween20 and incubated for 2 h at room temperature. Anti-MrkA antibody was detected using an alkaline phosphatase conjugated secondary antibody (Sigma-Aldrich) at a concentration of 1:30 000 in PBS + 0.05 Tween20 and incubated for 1 h at 37°C. Wells were developed using the substrate p-nitrophenyl phosphate (Sigma-Aldrich) (5 mg ml^{-1} in diethanolamine buffer) at room temperature for 15 min and enzymatic reactions were stopped using 3 N NaOH. Absorbances at 405 nm were determined using a microtitre plate reader.

Acknowledgements

We would like to thank Nora Cronin for help in X-ray data collection. ATR was supported by the Fundação para a Ciência e Tecnologia, Grant code SFRH/BD/22254/2005. This work was supported in part by Grant 85602 from MRC to GW, NIH Grant AI1050011 to SC and NIH training Grant T32 AI007511 to JGJ.

Accession numbers

The atomic co-ordinates of the MrkDrd have been deposited in the RCSB Protein Data Bank under Accession number 3U4K. The UniProtKB/Swiss-Prot Accession code for $MrkD_{1P}$ is P21648 and its GenBank Code is M24536.1.

References

Adams, P.D., Grosse-Kunstleve, R.W., Hung, L.W., Ioerger, T.R., McCoy, A.J., Moriarty, N.W., *et al.* (2002) PHENIX: building new software for automated crystallographic structure determination. *Acta Crystallogr D Biol Crystallogr* **58:** 1948–1954.

Allen, B.L., Gerlach, G.F., and Clegg, S. (1991) Nucleotide sequence and functions of mrk determinants necessary for expression of type 3 fimbriae in *Klebsiella* pneumoniae. *J Bacteriol* **173:** 916–920.

Bouckaert, J., Berglund, J., Schembri, M., De Genst, E., Cools, L., Wuhrer, M., *et al.* (2005) Receptor binding studies disclose a novel class of high-affinity inhibitors of the *Escherichia coli* FimH adhesin. *Mol Microbiol* **55:** 441–455.

Buts, L., Bouckaert, J., De Genst, E., Loris, R., Oscarson, S., Lahmann, M., *et al.* (2003) The fimbrial adhesin F17-G of enterotoxigenic *Escherichia coli* has an immunoglobulin-like lectin domain that binds N-acetylglucosamine. *Mol Microbiol* **49:** 705–715.

CCP4 (1994) The CCP4 suite: programs for protein crystallography. *Acta Crystallogr D Biol Crystallogr* **50:** 760–763.

Chen, V.B., Arendall, W.B., 3rd, Headd, J.J., Keedy, D.A., Immormino, R.M., Kapral, G.J., *et al.* (2010a) MolProbity: all-atom structure validation for macromolecular crystallography. *Acta Crystallogr D Biol Crystallogr* **66:** 12–21.

Chen, V.B., Arendall, W.B., 3rd, Headd, J.J., Keedy, D.A., Immormino, R.M., Kapral, G.J., *et al.* (2010b) MolProbity: all-atom structure validation for macromolecular crystallography. *Acta crystallographica. Section D, Biological crystallography* **66:** 12–21.

Clegg, S., and Gerlach, G.F. (1987) Enterobacterial fimbriae. *J Bacteriol* **169:** 934–938.

Dodson, K.W., Pinkner, J.S., Rose, T., Magnusson, G., Hultgren, S.J., and Waksman, G. (2001) Structural basis of the interaction of the pyelonephritic *E. coli* adhesin to its human kidney receptor. *Cell* **105:** 733–743.

Emsley, J., Knight, C.G., Farndale, R.W., Barnes, M.J., and Liddington, R.C. (2000) Structural basis of collagen recognition by integrin alpha2beta1. *Cell* **101:** 47–56.

Emsley, P., and Cowtan, K. (2004) Coot: model-building tools for molecular graphics. *Acta Crystallogr D Biol Crystallogr* **60:** 2126–2132.

Furthmayr, H., and Madri, J.A. (1982) Rotary shadowing of connective tissue macromolecules. *Coll Relat Res* **2:** 349–363.

Geibel, S., and Waksman, G. (2011) Crystallography and electron microscopy of chaperone/usher pilus systems. *Adv Exp Med Biol* **715:** 159–174.

Gerlach, G.F., Allen, B.L., and Clegg, S. (1989) Type 3 fimbriae among enterobacteria and the ability of spermidine to inhibit MR/K hemagglutination. *Infect Immun* **57:** 219–224.

Girardeau, J.P., and Bertin, Y. (1995) Pilins of fimbrial adhesins of different member species of *Enterobacteriaceae* are structurally similar to the C-terminal half of adhesin proteins. *FEBS Lett* **357:** 103–108.

Gouet, P., Courcelle, E., Stuart, D.I., and Metoz, F. (1999) ESPript: analysis of multiple sequence alignments in PostScript. *Bioinformatics* **15:** 305–308.

Holm, L., Kaariainen, S., Rosenstrom, P., and Schenkel, A. (2008) Searching protein structure databases with DaliLite v.3. *Bioinformatics* **24:** 2780–2781.

Hornick, D.B., Thommandru, J., Smits, W., and Clegg, S. (1995) Adherence properties of an mrkD-negative mutant of *Klebsiella pneumoniae*. *Infect Immun* **63:** 2026–2032.

Huang, Y.J., Liao, H.W., Wu, C.C., and Peng, H.L. (2009) MrkF is a component of type 3 fimbriae in *Klebsiella pneumoniae*. *Res Microbiol* **160:** 71–79.

Johnson, J.G., and Clegg, S. (2010) Role of MrkJ, a phosphodiesterase, in type 3 fimbrial expression and biofilm formation in *Klebsiella pneumoniae*. *J Bacteriol* **192:** 3944–3950.

Johnson, J.G., Murphy, C.N., Sippy, J., Johnson, T.J., and Clegg, S. (2011) Type 3 fimbriae and biofilm formation are regulated by the transcriptional regulators MrkHI in *Klebsiella* pneumoniae. *J Bacteriol* **193:** 3453–3460.

Kabsch, W. (1993) Automatic processing of rotation diffraction data from crystals of initially unknown symmetry and cell constants. *J Appl Crystallogr* **26:** 795–800.

Larkin, M.A., Blackshields, G., Brown, N.P., Chenna, R., McGettigan, P.A., McWilliam, H., *et al.* (2007) Clustal W and Clustal X version 2.0. *Bioinformatics* **23:** 2947–2948.

Martinez-Hernandez, A., Gay, S., and Miller, E.J. (1982) Ultrastructural localization of type V collagen in rat kidney. *J Cell Biol* **92:** 343–349.

Merckel, M.C., Tanskanen, J., Edelman, S., Westerlund-Wikstrom, B., Korhonen, T.K., and Goldman, A. (2003) The structural basis of receptor-binding by *Escherichia coli* associated with diarrhea and septicemia. *J Mol Biol* **331:** 897–905.

Modesti, A., Kalebic, T., Scarpa, S., Togo, S., Grotendorst, G., Liotta, L.A., and Triche, T.J. (1984) Type V collagen in human amnion is a 12 nm fibrillar component of the pericellular interstitium. *Eur J Cell Biol* **35:** 246–255.

Nuccio, S.P., and Baumler, A.J. (2007) Evolution of the chaperone/usher assembly pathway: fimbrial classification goes Greek. *Microbiol Mol Biol Rev* **71:** 551–575.

Ponnuraj, K., Bowden, M.G., Davis, S., Gurusiddappa, S., Moore, D., Choe, D., *et al.* (2003) A 'dock, lock, and latch' structural model for a staphylococcal adhesin binding to fibrinogen. *Cell* **115:** 217–228.

Pouttu, R., Puustinen, T., Virkola, R., Hacker, J., Klemm, P., and Korhonen, T.K. (1999) Amino acid residue Ala-62 in the FimH fimbrial adhesin is critical for the adhesiveness of meningitis-associated *Escherichia coli* to collagens. *Mol Microbiol* **31:** 1747–1757.

Saarela, S., Westerlund-Wikstrom, B., Rhen, M., and Korhonen, T.K. (1996) The GafD protein of the G (F17) fimbrial complex confers adhesiveness of *Escherichia coli* to laminin. *Infect Immun* **64:** 2857–2860.

Sebghati, T.A., and Clegg, S. (1999) Construction and characterization of mutations within the *Klebsiella* mrkD1P gene that affect binding to collagen type V. *Infect Immun* **67:** 1672–1676.

Sebghati, T.A., Korhonen, T.K., Hornick, D.B., and Clegg, S. (1998) Characterization of the type 3 fimbrial adhesins of *Klebsiella* strains. *Infect Immun* **66:** 2887–2894.

Tarkkanen, A.M., Allen, B.L., Westerlund, B., Holthofer, H., Kuusela, P., Risteli, L., *et al.* (1990) Type V collagen as the target for type-3 fimbriae, enterobacterial adherence organelles. *Mol Microbiol* **4:** 1353–1361.

Tarkkanen, A.M., Westerlund-Wikstrom, B., Erkkila, L., and Korhonen, T.K. (1998) Immunohistological localization of the MrkD adhesin in the type 3 fimbriae of *Klebsiella pneumoniae*. *Infect Immun* **66:** 2356–2361.

Westerlund, B., Kuusela, P., Risteli, J., Risteli, L., Vartio, T., Rauvala, H., *et al*. (1989a) The O75X adhesin of uropathogenic *Escherichia coli* is a type IV collagen-binding protein. *Mol Microbiol* **3:** 329–337.

Westerlund, B., Kuusela, P., Vartio, T., van Die, I., and Korhonen, T.K. (1989b) A novel lectin-independent interaction of P fimbriae of *Escherichia coli* with immobilized fibronectin. *FEBS Lett* **243:** 199–204.

Westerlund, B., van Die, I., Kramer, C., Kuusela, P., Holthofer, H., Tarkkanen, A.M., *et al*. (1991) Multifunctional nature of P fimbriae of uropathogenic *Escherichia coli*: mutations in fsoE and fsoF influence fimbrial binding to renal tubuli and immobilized fibronectin. *Mol Microbiol* **5:** 2965–2975.

Zong, Y., Xu, Y., Liang, X., Keene, D.R., Hook, A., Gurusiddappa, S., *et al*. (2005) A 'Collagen Hug' model for *Staphylococcus aureus* CNA binding to collagen. *EMBO J* **24:** 4224–4236.

Supporting information

Additional supporting information may be found in the online version of this article.